4-4-2016

Tidal Hydrodynamics Under Future Sea Level Rise and Coastal Morphology in the Northern Gulf of Mexico

Davina L. Passeri

Scott C. Hagen

Nathaniel G. Plant

Matthew V. Bilskie

Stephen C. Medeiros

See next page for additional authors

Publication Info

Published in *Earth's Fare*, Volume 4, Issue 5, 2016, pages 159-176.

AGU PUBLICATIONS

Earth's Future

RESEARCH ARTICLE
10.1002/2015EF000332

Special Section:
Integrated field analysis & modeling of the coastal dynamics of sea level rise in the northern Gulf of Mexico

Key Points:
- Tidal amplitudes in bays increase under SLR because of increases in inlet cross-sectional area
- Tidal velocities increase and flood/ebb dominance in tidal currents is altered under SLR
- Tidal propagation tends to be faster in future scenarios

Corresponding author:
D. L. Passeri, dpasseri@usgs.gov

Citation:
Passeri, D. L., S. C. Hagen, N. G. Plant, M. V. Bilskie, S. C. Medeiros, and K. Alizad (2016), Tidal hydrodynamics under future sea level rise and coastal morphology in the Northern Gulf of Mexico, *Earth's Future*, *4*, 159–176, doi:10.1002/2015EF000332.

Received 19 OCT 2015
Accepted 8 MAR 2016
Accepted article online 4 APR 2016
Published online 9 MAY 2016

Tidal hydrodynamics under future sea level rise and coastal morphology in the Northern Gulf of Mexico

Davina L. Passeri[1], Scott C. Hagen[2], Nathaniel G. Plant[1], Matthew V. Bilskie[3], Stephen C. Medeiros[4], and Karim Alizad[4]

[1]U.S. Geological Survey St. Petersburg Coastal and Marine Science Center, St. Petersburg, Florida, USA, [2]Department of Civil & Environmental Engineering, Center for Computation & Technology, Louisiana State University, Baton Rouge, Louisiana, USA, [3]Department of Civil & Environmental Engineering, Louisiana State University, Baton Rouge, Louisiana, USA, [4]Department of Civil, Environmental, and Construction Engineering, University of Central Florida, Orlando, Florida, USA

Abstract This study examines the integrated influence of sea level rise (SLR) and future morphology on tidal hydrodynamics along the Northern Gulf of Mexico (NGOM) coast including seven embayments and three ecologically and economically significant estuaries. A large-domain hydrodynamic model was used to simulate astronomic tides for present and future conditions (circa 2050 and 2100). Future conditions were simulated by imposing four SLR scenarios to alter hydrodynamic boundary conditions and updating shoreline position and dune heights using a probabilistic model that is coupled to SLR. Under the highest SLR scenario, tidal amplitudes within the bays increased as much as 67% (10.0 cm) because of increases in the inlet cross-sectional area. Changes in harmonic constituent phases indicated that tidal propagation was faster in the future scenarios within most of the bays. Maximum tidal velocities increased in all of the bays, especially in Grand Bay where velocities doubled under the highest SLR scenario. In addition, the ratio of the maximum flood to maximum ebb velocity decreased in the future scenarios (i.e., currents became more ebb dominant) by as much as 26% and 39% in Weeks Bay and Apalachicola, respectively. In Grand Bay, the flood-ebb ratio increased (i.e., currents became more flood dominant) by 25% under the lower SLR scenarios, but decreased by 16% under the higher SLR as a result of the offshore barrier islands being overtopped, which altered the tidal prism. Results from this study can inform future storm surge and ecological assessments of SLR, and improve monitoring and management decisions within the NGOM.

1. Introduction

Coasts are dynamic systems that continuously transform over different temporal and spatial scales as a result of geomorphic and oceanographic processes [*Cowell et al.*, 2003a, 2003b]. Sea level rise (SLR) has the potential to affect coastal environments in a multitude of ways including increased flooding, increased erosion, and changes in tidal flows and elevations that are important for maintaining estuarine form and function. Low-gradient coastal environments such as the Northern Gulf of Mexico (NGOM) are some of the most vulnerable areas to SLR in the continental United States [*Thieler and Hammar-Klose*, 1999], which may have serious consequences for coastal communities and habitats. The Gulf coast attracts millions of residents, visitors, and businesses [*Florida Department of Environmental Protection*, 2013] and contains ecologically and economically significant wetlands and habitats with an estimated commercial harvest value of $779 million in 2012 [*National Marine Fisheries Service*, 2013]. Understanding the future value of these coastal environments relies on the scientific evaluation of risks associated with SLR. This understanding can be used to make informed decisions for managing human and natural communities.

Changes in tidal hydrodynamics under SLR may impact navigation, ecological habitats, infrastructure, and the geomorphology of the coastline. Specifically, tidal hydrodynamics influences inundation, circulation, and sediment transport processes. Previous studies have found that SLR may cause nonlinear increases in tidal ranges and tidal prisms, and may alter inundation, current velocities, and circulation patterns in the nearshore environment [*French*, 2008; *Leorri et al.*, 2011; *Pickering et al.*, 2012; *Hall et al.*, 2013; *Pelling et al.*, 2013; *Valentim et al.*, 2013; *Arns et al.*, 2015]. In addition, long-term shoreline erosion rates are expected to increase under future SLR [*Gutierrez et al.*, 2011], which may have consequences for barrier islands

and coastal embayments. Despite knowledge of the dynamic nature of the coast, many hydrodynamic assessments of SLR have not accounted for future changes in coastal morphology, which may increase inundation and alter hydrodynamics [*Bilskie et al.*, 2014; *Passeri et al.*, 2015a, 2015b]. Furthermore, most hydrodynamic assessments have been concentrated on a localized study area (e.g., a single estuary). This study aims to have a broader synthesis of SLR impacts evaluated across a broad domain with multiple embayments.

The NGOM is ideal for examining SLR impacts on tidal hydrodynamics because it includes a variety of estuaries with different geometries, tidal forcing, and geomorphic settings. This study examines the integrated dynamic effects of SLR and projected morphology on tidal hydrodynamics along embayments in the NGOM coast with particular focus on the Apalachicola, Florida (FL), Grand Bay, Mississippi (MS), and Weeks Bay, Alabama (AL) National Estuarine Research Reserves (NERRs). A large-domain hydrodynamic model was used to simulate astronomic tides for present and future conditions (circa 2050 and 2100). The future conditions included four SLR scenarios and corresponding changes of shoreline positions and dune elevations. While the analysis herein is focused primarily on the three NERRs, notable changes in tidal parameters in the other bay systems or offshore are also explored. Changes in harmonic constituent amplitudes and phases, current velocities, and inundation extents are estimated to measure the sensitivity of the tidal hydrodynamic response to SLR under a changing landscape.

2. Study Domain

The domain for this study spans the Chandeleur Islands, Louisiana (LA) through Apalachicola, FL, including seven embayments (Mississippi Sound, Mobile Bay, Perdido Bay, Pensacola Bay, Choctawhatchee Bay, St. Andrew Bay, and Apalachicola Bay), numerous barrier islands and a stretch of mainland beach (Figure 1). This section of the NGOM is a low wave energy, microtidal environment with an average wave height and tidal range on the order of 0.5 m and less than 1 m, respectively. Astronomic tides change from being mixed semi-diurnal along the west coast of Florida, to mixed diurnal at Apalachicola Bay, to diurnal along the Florida Panhandle through Louisiana [*Seim et al.*, 1987]. Shorelines along this stretch of the NGOM coast are currently eroding horizontally at rates exceeding 2 m/year (LA) or are nearly stable (FL) [*Morton et al.*, 2004]; however, over the past 6000 years, the coast has not experienced the rates of SLR that are projected for the next century [*Donoghue*, 2011].

The Apalachicola, Grand Bay, and Weeks Bay NERRs are of particular interest because of their economic and ecologic importance in the NGOM. Each estuary has its own unique morphology and hydrodynamic influences. Therefore, it is likely that each NERR will respond differently to SLR. Apalachicola is a wide, shallow estuary located within the Florida Panhandle. It is the second largest watershed system in the NGOM surpassed only by the Mobile River basin [*Isphording*, 1985]. The estuary is centered on Apalachicola Bay, with East Bay to the northeast. The Apalachicola River discharges into East Bay through a delta and distributary system nearly 3 km wide. The estuary is sheltered from the Gulf of Mexico by a chain of barrier islands. Apalachicola is an ecologically and economically significant estuary that contains oyster reefs, seagrass beds, and salt marshes. Oysters, shrimp, blue crab, and finfish are the most harvested species with a value over $134 million in economic impact annually. In addition, Apalachicola Bay provides approximately 90% of Florida's oyster harvest and 10% of the total U.S. harvest [*FDEP*, 2013].

Grand Bay is located within the Mississippi Sound on the Mississippi-Alabama (MSAL) border. It is comprised of multiple bays, bayous, and salt marshes. Salt marshes provide habitats for many species, including shrimp, crabs, and oysters that are recreationally and commercially fished. The estuary is one of the few remaining extensive coastal marsh environments in Mississippi [*O'Sullivan and Criss*, 1998] and is being eroded away faster than any other marsh in the state [*Mississippi Department of Marine Resources*, 1999]. Currently, the estuary does not have a fluvial source, and is solely influenced by the hydrodynamics of the Mississippi Sound. The historic breaching and migration of the offshore MSAL barrier islands have altered tidal hydrodynamics within the Mississippi Sound and Grand Bay estuary [*Eleuterius and Criss*, 1991; *Passeri et al.*, 2015a]. Lack of a sediment source and reduced protection from wave attack have heightened the susceptibility of the estuary's marsh shorelines to increased erosion under SLR. In addition, as the offshore barrier islands continue to evolve, tidal hydrodynamic patterns within Grand Bay may be further altered.

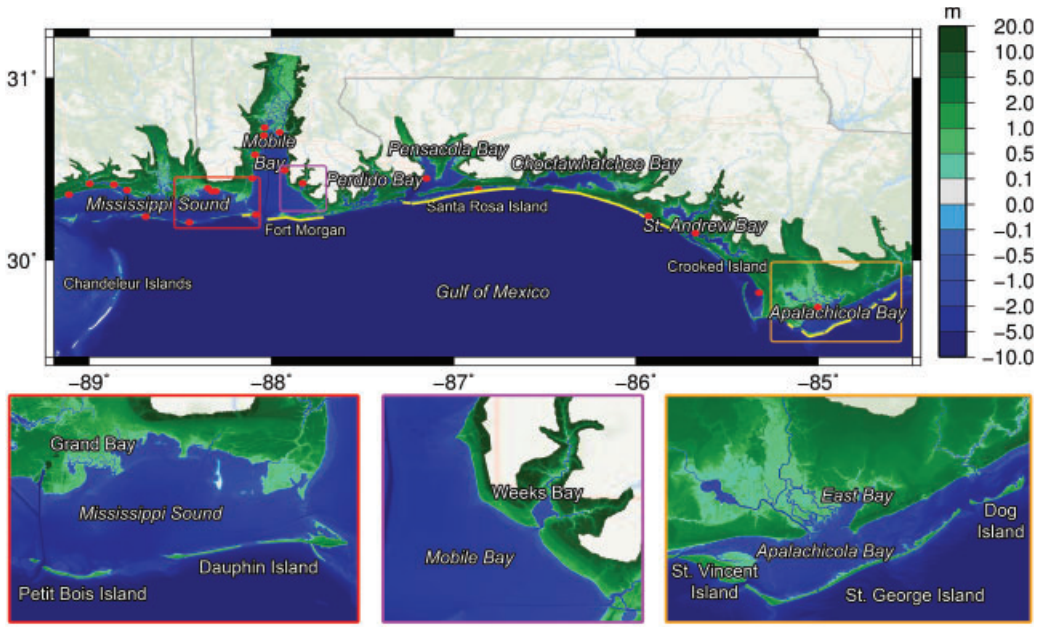

Figure 1. Hydrodynamic model elevations of the Northern Gulf of Mexico study area with insets of the Grand Bay, Weeks Bay, and Apalachicola National Estuarine Research Reserves; red dots indicate locations of National Oceanographic and Atmospheric Administration tide gauge stations used to validate the hydrodynamic model; yellow shorelines indicate regions where the Bayesian network projected shoreline change (Figure 2) exceeded the barrier island width or infrastructure line and were therefore assumed to be nourished under future scenarios based on Figure 3.

Weeks Bay is considered a tributary estuary and is located within the larger estuary system of Mobile Bay, which connects Weeks Bay to marine influences of the Gulf of Mexico. Weeks Bay receives tidal flows from Mobile Bay as well as freshwater discharge from the Fish and Magnolia Rivers. The estuary supports diverse species of flora and fauna, and is a particularly important nursery for commercially significant species including shrimp, bay anchovy, blue crab, and shellfish [*Miller-Way et al.*, 1996].

3. Methodology

To assess changes in tidal inundation, amplitudes, phases, and current velocities because of SLR, four SLR scenarios from recent climate assessments and coupled morphologic changes were selected to drive a high-resolution hydrodynamic model constructed for the study domain.

3.1. Future SLR Scenarios

Future sea levels were obtained from the *Parris et al.* [2012] scenarios for low, intermediate-low, intermediate-high, and high global projections of SLR for the years 2050 (0.11, 0.19, 0.39, 0.62 m of SLR, respectively) and 2100 (0.2, 0.5, 1.2, 2.0 m of SLR, respectively). The low scenario was derived from a linear extrapolation of historical mean SLR using tide gauge records dating back to 1900. The intermediate-low scenario was determined using the upper end of the IPCC Fourth Assessment Report (AR4) global SLR projections from climate models employing the B1 emissions scenario [*Intergovernmental Panel on Climate Change*, 2007]; the intermediate-high scenario was derived from the average of the high end of semi-empirical global SLR projections, and the highest projection was determined using estimates of maximum possible glacier and ice sheet loss and estimated ocean warming from the IPCC AR4 global SLR projection. These scenarios are considered to be plausible trajectories of global mean SLR for use in assessing vulnerability, impacts, and adaption strategies [*Parris et al.*, 2012].

3.2. Hydrodynamic Model

To simulate tidal hydrodynamics, this study uses ADCIRC-2DDI, a code that solves the depth-integrated shallow water equations for water surface elevations and currents [*Luettich et al.*, 1992]. The model is a compilation of three previously developed models [*Bilskie et al.*, 2015b]. The unstructured finite element mesh

describes the Western North Atlantic Tidal model domain west of the 60°W meridian (open ocean boundary), including the Caribbean Sea and the Gulf of Mexico. Higher spatial resolution elements (on the order of 20–100 m) are incorporated along the NGOM coast from Louisiana through the Florida panhandle, which permits localized adjustments to be made to support the simulation of future scenarios with changes in shorelines and other morphology. Bathymetric and topographic elevations were derived from a digital elevation model (DEM) constructed with lidar data, as well as National Ocean Service (NOS) hydrographic surveys, U.S. Army Corps of Engineers (USACE) channel surveys and National Oceanographic and Atmospheric Administration (NOAA) nautical charts to represent present conditions post-Katrina; the last major hurricane to directly affect this portion of the NGOM [*Coggin*, 2011; *Bilskie et al.*, 2015a]. Because Apalachicola and Grand Bay have extensive marsh regions and are of particular interest in this study, an elevation correction based on biomass density was employed to adjust the lidar-derived elevations. This technique uses ASTER (Advanced Spaceborne Thermal Emission and Reflection Radiometer) and IfSAR (interferometric synthetic aperture radar) satellite imagery along with lidar-derived canopy heights to classify the above-ground biomass density as high, medium, or low. This biomass density class was then used to lower the lidar DEM [*Medeiros et al.*, 2015].

3.3. Morphologic Model

Projecting long-term changes in coastal morphology is challenging because of the stochastic nature of the processes, in particular the uncertainty in frequency and magnitude of storms, as well as a lack of understanding in the dynamic interactions and feedback mechanisms [*Sampath et al.*, 2011]. As a result, coastal scientists do not have a reliable, universal model to accurately predict the impacts of SLR along a variety of coastlines [*Fitzgerald et al.*, 2008]. Statistical approaches using Bayesian networks (BNs) have been used to make probabilistic predictions of long-term shoreline change that depend on SLR [*Hapke and Plant*, 2010; *Gutierrez et al.*, 2011; *Yates and Le Cozannet*, 2012]. The BN, based on the application of Bayes' theorem, defines relationships between driving forces, geological constraints, and coastal responses [*Gutierrez et al.*, 2011]. In this study, an existing BN [*Gutierrez et al.*, 2014] was modified to project future shoreline changes and dune heights along the NGOM coast under each SLR scenario [*Plant et al.*, 2015]. To do so, the SLR rate variable was constrained in the BN and probabilistic projections of shoreline change and dune heights were output at 4 km sections along the oceanic shorelines of the NGOM coast. The BN was beneficial in this application because it could be applied to a large domain with minimal computational expense. The BN is trained on historical data including observed, relative SLR, and can represent probabilities of shoreline and dune-height changes that are consistent with future SLR. This probabilistic approach folds in a variety of processes, including storms and long-term changes because of alongshore and cross-shore sediment transport that are correlated to broad-scale hydrodynamic and geomorphic conditions including SLR, wave height, tide range, and geomorphic setting. However, the spatial applicability of the BN was limited to oceanic shorelines because of a lack of data in bay and estuarine regions. There was also a limited level of detail in which the BN could make projections; predictions were bound by what the BN had seen historically (e.g., the rate of SLR), and the BN was unable to explicitly represent complex morphological processes such as barrier island translation or rollover (e.g., how the back-barrier shoreline would be altered). While a range of morphologic scenarios were predicted for each SLR scenario [*Plant et al.*, 2015], a single, most likely scenario was extracted to use in the hydrodynamic model; the 50th percentile projections of shoreline change and dune heights were selected to represent an "average" projection of future morphology. Because the BN was not trained with SLR rates as large as the high SLR scenario, it was only able to output projections for the low, intermediate-low, and intermediate-high scenarios. To obtain projections under the high SLR scenario, the shoreline change and dune elevations predicted by the BN for the low, intermediate-low, and intermediate-high projections were linearly extrapolated (Figure 2). The majority of the NGOM shoreline was projected to erode, although some areas were projected to accrete especially near inlets. In general, as SLR increased, shoreline erosion increased and dune elevation decreased.

3.4. Modeling Approach

To examine the effects of SLR on tidal hydrodynamics along the NGOM coast, the hydrodynamic model was altered to reflect future conditions circa 2050 and 2100 (note: morphologic processes were not simulated concurrently with hydrodynamics as the goal was to simulate tidal hydrodynamics in response to SLR and

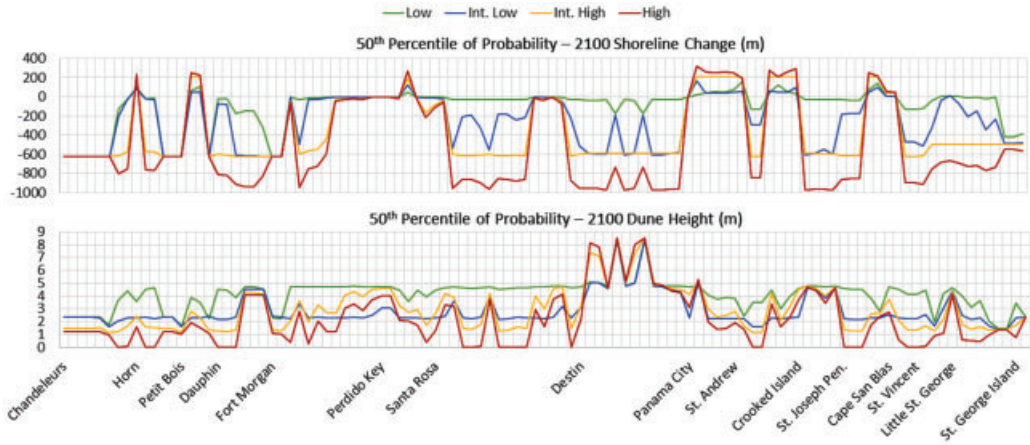

Figure 2. Fiftieth percentile of probability projections of shoreline change and dune height for the year 2100 under low, intermediate-low, intermediate-high, and high sea level rise across the Northern Gulf of Mexico domain. In the plot of shoreline change, positive numbers indicate accretion, negative numbers indicate erosion. The horizontal scale corresponds to 4 km longitude per grid mark.

landscape changes). To do so, the DEM was altered using the BN output to represent future elevations. In order to account for the dynamic movement of the shoreface, the beach profile was translated upwards by the amount of SLR, and landwards or seawards by the amount of projected erosion or accretion, while maintaining the profile shape (i.e., equilibrium) [*Passeri et al.*, 2015b]. The profile translation was implemented for each 4 km section by shifting the active zone portion of the DEM, defined from the shoreline (0 m contour) to the depth of closure contour (estimated to be approximately 5 m along the coastline [*Dean and Grant*, 1989]). Bathymetry and topography outside of the active zone remain the same. Dune heights were then modified using the corresponding BN output.

At many locations, the BN-projected shoreline was landward of infrastructure, and/or exceeded the position of the back-barrier shoreline (i.e., the shoreline change exceeded the width of the barrier island). Because the BN was unable to project how the back-barrier shoreline would be altered, it was unable to provide guidance on how the entire barrier island would evolve. To compensate for this short-coming, a decision-making flowchart was created to decide how to implement the BN-projected shoreline changes into the hydrodynamic model based on the assumptions of whether shorelines (as indicated in Figure 1) would be nourished in the future to prevent barrier island or infrastructure loss (Figure 3). A step-by-step explanation of the flowchart follows:

1. At accretional sections, the beach profile was translated according to the projected shoreline change and the dune height was altered.
2. At erosional sections, if the projected shoreline position was landward of the back-barrier shoreline and section was an urban area, it was assumed that the shoreline would be nourished in the future. Therefore, the shoreline position was not altered (i.e., horizontal translation was set equal to 0), the beach profile was shifted vertically by the amount of SLR, and the dune height was changed according to the projection.
3. At erosional sections, if the projected shoreline position was landward of the back-barrier shoreline and the section was not an urban area, then, USGS land use/land cover projections for the years 2050 and 2100 using the A2 scenario (http://landcover-modeling.cr.usgs.gov/projects.php) were consulted to determine if the area was projected to be developed.
   (a) If there was projected development, it was assumed that the shoreline would be nourished in the future; the shoreline position was not altered, the beach profile was shifted vertically by the amount of SLR and the dune height was changed according to the projection.
   (b) If there was not projected development but the section was state or government property (e.g., military base, state/national park, etc.), then it was assumed that the shoreline would be nourished in the future; the shoreline position was not altered, the beach profile was shifted vertically by the amount of SLR the dune height was changed according to the projection.

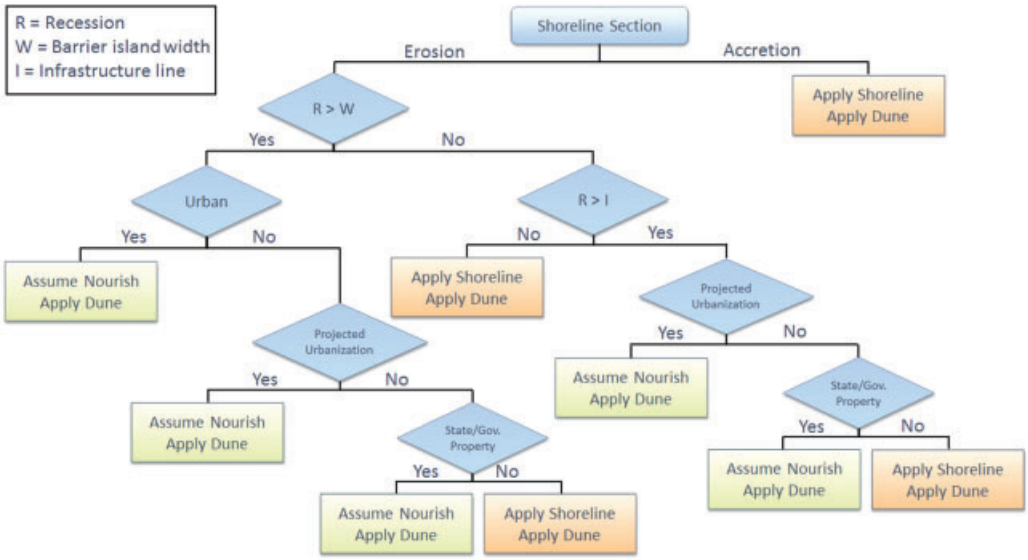

Figure 3. Decision making flow chart for how to implement projected shoreline changes and dune heights from BN into hydrodynamic model.

(c) If there was not projected development and the section was not state or government property, then the beach profile was translated according to the projected shoreline change and the dune height was altered.

4. If the projected shoreline position was not landward of the back-barrier shoreline and did not exceed the infrastructure line, then the beach profile was translated according to the projected shoreline change and the dune height was altered.
5. If the projected shoreline change exceeded the infrastructure line, then the same methodology for if the shoreline projection was landward of the back-barrier shoreline was applied.

As previously mentioned, the morphology of the MSAL barrier islands influences hydrodynamic patterns within the Mississippi Sound and Grand Bay [*Passeri et al.*, 2015a]. To account for future lateral migration of the islands, historic migration rates were extrapolated to the years 2050 and 2100, and used to modify elevations in the DEM. The western end of Dauphin Island has grown laterally at an average rate of 45.7 m/year, whereas the eastern end is fixed by its Pleistocene core [*Morton*, 2008; *Rosati and Stone*, 2009; *Byrnes et al.*, 2012]. Petit Bois Island has migrated westward at an approximate rate of 34.5 m/year with net erosion on the eastern end, that has widened the pass to Dauphin Island. The western end of Petit Bois Island is prevented from migrating further westward because of the maintained shipping channel at Horn Island pass [*McBride et al.*, 1995; *Morton*, 2008]. Horn Island has migrated westward at a rate of approximately 38.7 m/year and Ship Island has migrated westward at approximately 9 m/year. Cat Island has remained relatively stable historically [*Morton*, 2008]; therefore, the island's morphology was not altered.

Astronomic tides were simulated for nine scenarios in which the sea level, shoreline positions, and dune elevations reflect the conditions for each time: present, 2050-low, 2050-intermediate low, 2050-intermediate high, 2050-high, 2100-low, 2100-intermediate low, 2100-intermediate high, and 2100-high. Astronomic tides were simulated for 45 days beginning from a cold start with a 10-day hyperbolic tangent ramp function. For the present scenario, the model was forced with water surface elevations of eight harmonic constituents (K_1, O_1, M_2, S_2, N_2, K_2, Q_1, and P_1) along the open ocean boundary [*Egbert et al.*, 1994; *Egbert and Erofeeva*, 2002]. For the future scenarios, a ninth "steady" component with zero-phase and an amplitude equal to the SLR projection for the given scenario was included to increase the sea level. Wind effects were not considered in this study, as preliminary research has shown that wind effects average out on an annual scale. Model output consisted of depth-integrated velocities, amplitudes, and phases of harmonic constituents, as well as maximum elevations of water and maximum velocities obtained at each node of the mesh for the duration of each simulation.

4. Results

4.1. Validation

The hydrodynamic model was validated with available astronomic tide data. A tidal validation was performed for the present scenario at 26 NOAA tide gauges located throughout the study domain (Figure 1). Model output consisted of 23 tidal constituents, which were validated against reported tidal constituents at each of the tidal gauging stations (http://tidesandcurrents.noaa.gov/). A comparison of the NOAA-predicted and model-computed amplitudes and phases for five dominant constituents (K_1, O_1, M_2, Q_1, and S_2) is shown in Figure 4. Difference bands are plotted at ±0.025 and ±0.05 m in the amplitude plots, and ±10° and ±20° in the phase plots. All of the constituent amplitudes fall within the 0.05 m difference band with an overall root mean square error (RMSE) of 5.04 cm. For the 11 stations in MS, the nine stations in AL and the six stations in FL, the RMSEs were 4.90, 4.30, and 5.96 cm, respectively. The stations with the lowest RMSEs (on the order of 3 cm) are located along the MSAL barrier islands. The phases of the three most dominant constituents (K_1, O_1, and M_2) fall within the 20° difference band for the most part. Although the S_2 phases deviate the most, the contribution of this constituent is minimal in comparison with K_1, O_1, and M_2. A more thorough discussion on model validation can be found in *Bilskie et al.* [2015b].

4.2. Water Levels

Tidal amplitudes (i.e., the amplitude of the tide with respect to mean sea level) across the NGOM for the present scenario are summarized in Figure 5a. Within the study domain, Apalachicola Bay had the highest tidal amplitudes (approximately 55 cm) as a result of the strong semi-diurnal influence. As the Gulf of Mexico becomes more diurnal westward of Apalachicola, tidal amplitudes generally decrease. Out of all of the embayments, Perdido and Choctawhatchee had the lowest tidal amplitudes (on the order of 21 and 15 cm, respectively) because of the bays being connected to the Gulf of Mexico with narrow, shallow inlets that limit tidal exchange.

Changes in tidal amplitudes from the present scenario to the future scenarios were examined; the present versus 2050-high and present versus 2100-high comparisons are summarized in Figure 5. Differences equal to 0 indicate that the tidal amplitude did not change from the present scenario, differences greater than 0 indicate that the tidal amplitude increased from the present scenario; differences less than 0 indicate that the tidal amplitude decreased from the present scenario. In all of the scenarios, the offshore tidal amplitudes were unaltered, illustrating the nonlinear effects of SLR within semi-enclosed embayments. In the present versus 2050-low scenario, no changes occurred within any of the bays. Similarly, changes were minimal in the 2100-low scenario with increases only in Perdido Bay and Choctawhatchee Bay of approximately 9% (1.9 cm) and 8% (1.2 cm), respectively; these increases are within the error of the hydrodynamic model. In the 2050-high scenario, tidal amplitudes increased from the present scenario by approximately 9% (3.5 cm), 23% (4.8 cm), and 26% (11.9 cm) in Mobile Bay/Weeks Bay, Perdido Bay, and Choctawhatchee Bay, respectively. The most substantial changes occurred in the 2100-high scenario with increases of 15% (6.5 cm), 35% (7.3 cm), 67% (10.0 cm), and 8% (5.5 cm) in Mobile Bay/Weeks Bay, Perdido Bay, Choctawhatchee Bay, and Apalachicola Bay, respectively. Pensacola Bay and St. Andrew Bay had negligible changes (less than 2%), which are also within the error of the hydrodynamic model.

Previous research has illustrated the relationship between inlet cross-sectional area (at high tide) and tidal prisms (i.e., the amount of water flowing into a bay during high tide) [*Jarrett*, 1976]. As sea level rises, the inlet cross-sectional area increases because of higher water levels; this assumes that the inlet bathymetry remains constant which is a valid assumption given that the aforementioned inlets are either hardened with coastal structures or dredged The relative change in the inlet cross-sectional area, measured across the narrowest cross-section of each inlet, versus the amount of SLR is plotted in Figure 6 for each bay that is connected to the Gulf of Mexico with a single inlet (i.e., Mobile, Perdido, Pensacola, Choctawhatchee, and St. Andrew). Under the 2100-high scenario, Choctawhatchee Bay had the largest relative increase in the inlet cross-sectional area by approximately 78%, whereas St. Andrew Bay had the smallest by approximately 20%. Trendlines fitted to the data can be used to project the relative change in the inlet cross-sectional area in each bay under various SLR scenarios that are less than or equal to 2 m. As the inlet geometry changes under SLR, the tidal hydrodynamic behavior within the bay is altered. The correlation between the ratio of the future to present tidal amplitude ($Amplitude_{future}/Amplitude_{present}$) and the ratio of the future to present inlet cross-sectional area ($Area_{future}/Area_{present}$) for each SLR scenario is summarized in Table 1. As

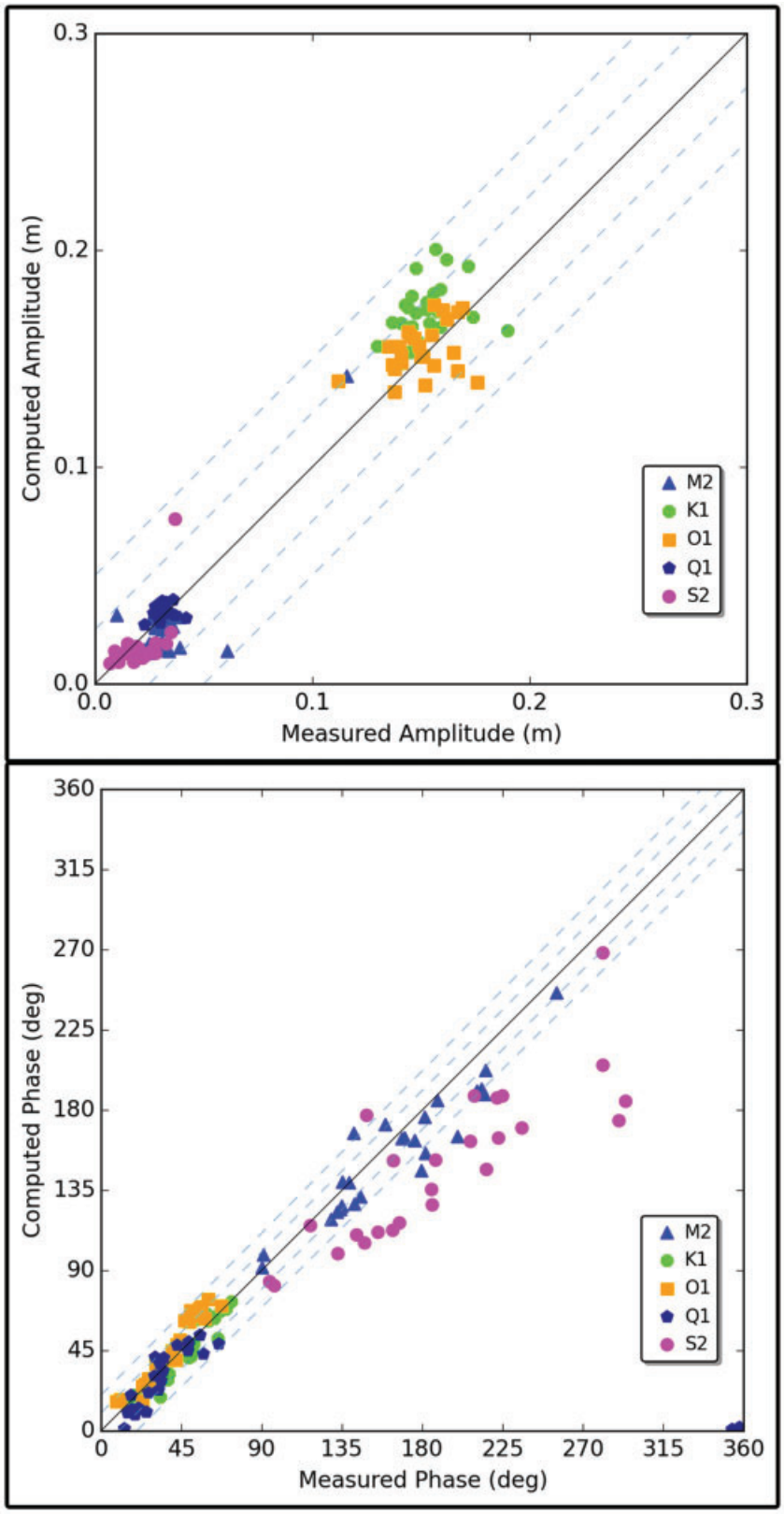

Figure 4. Comparison of harmonic constituent amplitudes (top) and phases (bottom) measured by National Oceanographic and Atmospheric Administration and predicted by the hydrodynamic model in the Northern Gulf of Mexico study area. Difference bands are located at 0.025 and 0.05 m in the amplitude plot, and 10° and 20° in the phase plot.

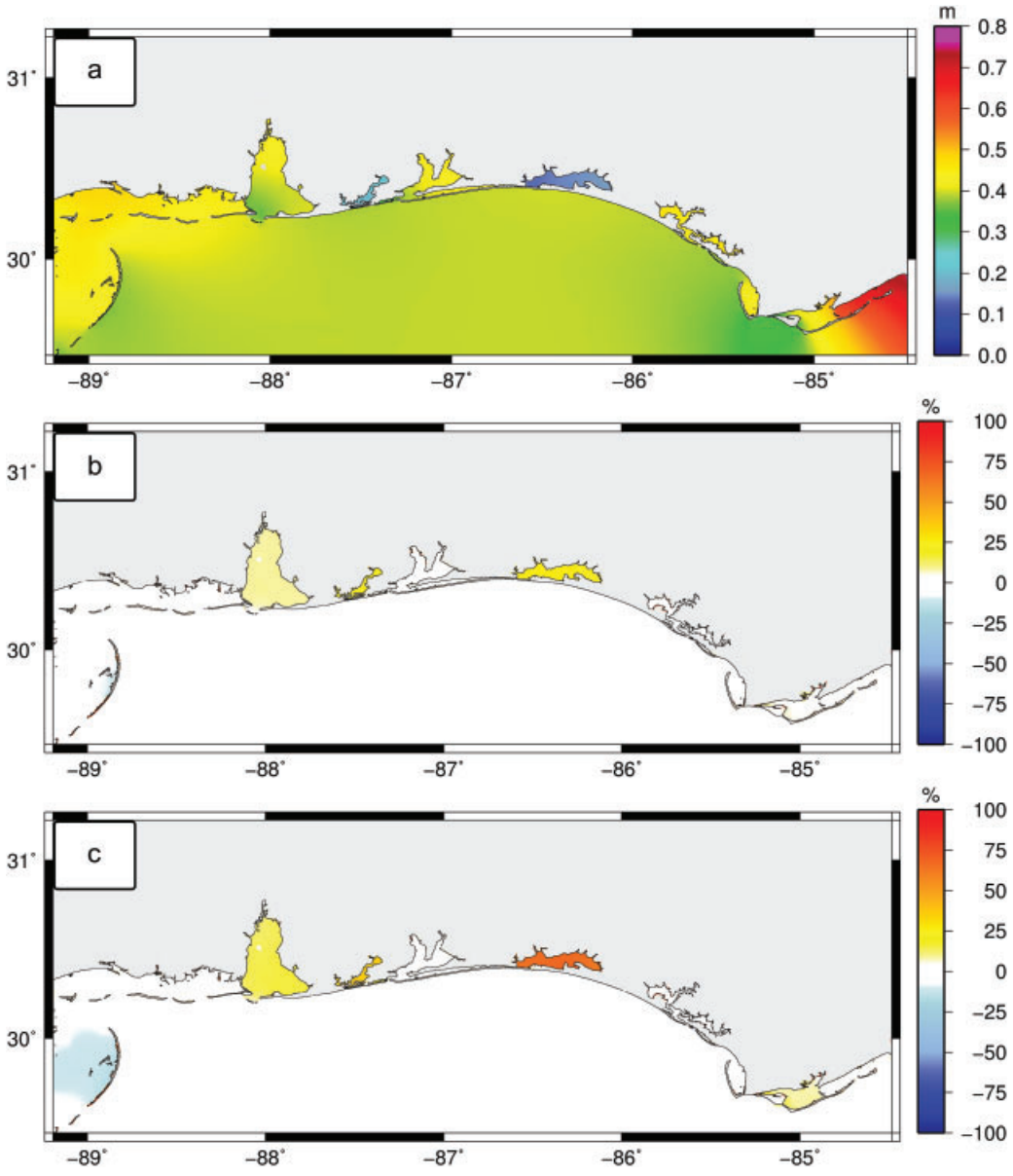

Figure 5. (a) Total tidal amplitudes across the Northern Gulf of Mexico study area for the present scenario; (b) percent change in tidal amplitude from present to 2050-high scenario; (c) percent change in tidal amplitude from present to 2100-high scenario.

evident by the high correlation coefficients (R), there is a strong linear correlation between the change in the inlet cross-sectional area and the change in the bay's tidal amplitude for each SLR scenario. Therefore, knowledge of how the inlet cross-sectional area of each bay will change under a certain SLR scenario (i.e., Figure 6) informs the resulting change in the tidal amplitude of the bay; the larger the increase in the inlet cross-sectional area, the larger the increase in the tidal amplitude.

Unlike the semi-enclosed embayments in the study domain, changes in tidal amplitudes within the Mississippi Sound and Grand Bay were negligible in all future scenarios because of the Sound's open exposure to the Gulf of Mexico. As a result, SLR did not alter the tidal amplitude response. Tidal amplitudes in the embayment west of the Chandeleur Islands decreased by approximately 11% (5.7 cm) in the 2100-high scenario as a result of the islands being overtopped, which created direct exposure to the Gulf of Mexico. This dampened the tidal response and caused the tidal hydrodynamic behavior in the embayment to be more similar to the open ocean.

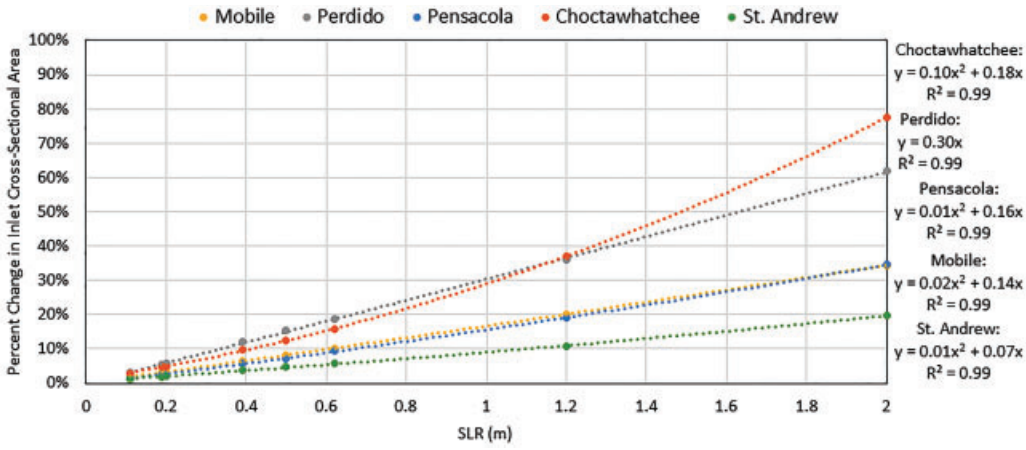

Figure 6. Percent change in inlet cross-sectional area versus sea level rise for each bay; data are fitted with trend equations.

Table 1. Trend Equations, Correlation Coefficient (R), and Coefficient of Determination (R^2) Between the Ratio of the Future to Present Tidal Amplitude ($Amplitude_{future}/Amplitude_{present}$) Versus the Ratio of the Future to Present Inlet Cross-Sectional Area ($Area_{future}/Area_{present}$) for Each Future Scenario in the NGOM Study Area

Scenario	Trendline	R	R^2
2050 Low	$y = 2.66x - 1.69$	0.99	0.99
2050 Int. low	$y = 2.55x - 1.60$	0.99	0.99
2050 Int. high	$y = 2.21x - 1.29$	0.97	0.93
2050 High	$y = 2.16x - 1.30$	0.93	0.86
2100 Low	$y = 2.50x - 1.55$	0.99	0.99
2100 Int. low	$y = 2.19x - 1.30$	0.96	0.92
2100 Int. high	$y = 1.43x - 0.62$	0.94	0.89
2100 High	$y = 1.15 - 0.42$	0.97	0.97

NGOM, Northern Gulf of Mexico.

To further examine the influence of SLR and morphology on tidal amplitudes, changes in the dominant tidal constituents were examined. The present dominant tidal constituent amplitudes as well as changes in constituent amplitudes and phases from present to the 2100-high scenario are summarized in Table 2. The dominant tidal constituents within the NGOM are the diurnal K_1 and O_1, as well as the semi-diurnal M_2. K_1 and O_1 dominate in the diurnal section of the NGOM, including the Mississippi Sound, Grand Bay, Mobile Bay, Weeks Bay, Perdido Bay, Pensacola Bay, Choctawhatchee Bay, and St. Andrew Bay. K_1, O_1, and M_2 dominate in Apalachicola Bay as a result of the strong semi-diurnal influence. In the diurnal bays, large increases in the K_1 and O_1 amplitudes contributed to the total increase in the tidal amplitude; although the M_2 amplitudes also changed, the change was small relative to the total tidal amplitude. As expected, Choctawhatchee and Perdido bays had the largest increases in the K_1 and O_1 amplitudes. In Apalachicola Bay, the O_1 and K_1 constituents increased minimally, whereas the M_2 constituent increased by 31.2% (3.7 cm), further illustrating the semi-diurnal nature of the tides in Apalachicola.

The phases of the dominant constituents (i.e., the phase lag) also changed from the present scenario to the 2100-high scenario. In all of the bays except St. Andrew Bay, constituent phases were faster in the 2100-high scenario than in the present scenario, meaning that high tide would occur earlier than in the present. The largest phase differences occurred in Weeks Bay, with the K_1 and O_1 phases being 116 and 134 min faster in the 2100-high scenario, respectively. In St. Andrew Bay, the K_1 and O_1 phases were slower in the 2100-high scenario by approximately 14.7 and 14.1 min, respectively. St. Andrew Bay had the smallest relative increase in the cross-sectional area of the inlet under the 2100-high scenario and experienced slower tidal propagation in the future scenario than in the present. On the contrary, bays with larger relative

Table 2. Dominant Harmonic Constituent Amplitudes for the Present Scenario and Changes in Constituent Amplitudes and Phases From the Present Scenario to the 2100-High Scenario Within Each Bay System in the NGOM Study Area

	Present Amplitude (cm)			% Change in Amplitude From Present to 2100-High			Difference in Phase From Present to 2100-High (min)		
Location	K_1	O_1	M_2	K_1 (%)	O_1 (%)	M_2 (%)	K_1	O_1	M_2
Mississippi Sound	17.8	16.2	2.5	−4.4	−3.8	5.8	19.9	23.7	11.3
Grand Bay	17.0	15.8	2.4	−2.4	−2.1	10.5	23.1	27.3	15.2
Mobile Bay	16.2	14.3	1.4	7.4	9.5	87.6	90.4	102.3	22.1
Weeks Bay	16.4	14.5	1.4	9.7	11.6	88.6	116.8	134.6	−9.2
Perdido Bay	7.9	7.0	0.6	37.1	39.2	12.5	76.1	86.7	14.8
Pensacola Bay	17.3	15.5	2.0	0.0	1.0	−6.9	44.2	54.4	88.4
Choctawhatchee Bay	5.7	5.0	0.4	70.7	73.6	35.8	86.3	92.8	22.8
St. Andrew Bay	16.4	15.3	2.8	0.9	−0.7	−25.2	−14.7	−14.6	−44.7
Apalachicola Bay	15.5	14.2	12.0	1.2	0.4	31.2	58.5	68.9	35.7

NGOM, Northern Gulf of Mexico.

increases in the cross-sectional area of the inlets experienced faster tidal propagation in the future scenario than in the present. Similar to the tidal amplitudes, no differences in the constituent phases occurred offshore.

4.3. Currents

Changes in maximum tidal current velocities from the present scenario to the future scenarios were compared; the changes from the present scenario to the 2050-high and 2100-high scenarios are summarized in Figure 7. Differences equal to 0 indicate that the maximum velocity did not change from the present scenario; differences greater than 0 indicate that the maximum velocity increased from the present scenario; differences less than 0 indicate that the maximum velocity decreased from the present scenario.

The present maximum tidal current velocities varied across the domain with faster velocities in the semi-diurnal region as well as within the inlets to the embayments; within the Mississippi Sound, tidal velocities were faster within the inlets of the barrier islands (up to 30 cm/s). Within the three NERRs, the present maximum tidal velocities at the locations specified in Figure 8 were 6.1, 4.1, and 17.4 cm/s in Grand Bay, Weeks Bay, and East Bay (Apalachicola), respectively. In the 2050-low scenario and the 2100-low scenarios, the only notable changes occurred in the Mississippi Sound within the present and future locations of the inlets of the offshore barrier islands. The westward migration of the barrier islands shifted the location of the strong velocities within the inlets. In the 2050-high scenario, velocities minimally increased in Grand Bay and Apalachicola Bay. Westward of the Chandeleur Islands, velocities decreased along the northern end as a result of the barrier islands being overtopped and hydrodynamics within the embayment becoming more like the open ocean. Within the rest of the domain, changes were negligible except offshore of Pensacola Bay where velocities increased by approximately 3 cm/s (88%) along the continental shelf break. In the 2100-high scenario, larger changes occurred across the domain and within the embayments. Westward of the northern Chandeleur Islands, tidal velocities decreased by approximately 16 cm/s; this also occurred north of Dauphin Island in the Mississippi Sound as a result of the barrier island being overtopped. Tidal velocities increased within all of the bays; within the NERRs, velocities increased by approximately 6.1 cm/s (102%) in Grand Bay, 1.7 cm/s (39%) in Weeks Bay, and 10.8 cm/s (63%) in East Bay (Apalachicola). In addition, velocities increased offshore along the continental shelf break. The largest increase (approximately 18 cm/s) occurred offshore of Pensacola Bay where the slope of the shelf break is steep (i.e., greater depths, faster) whereas smaller increases (of approximately 6 cm/s) occurred where the slope is more gradual.

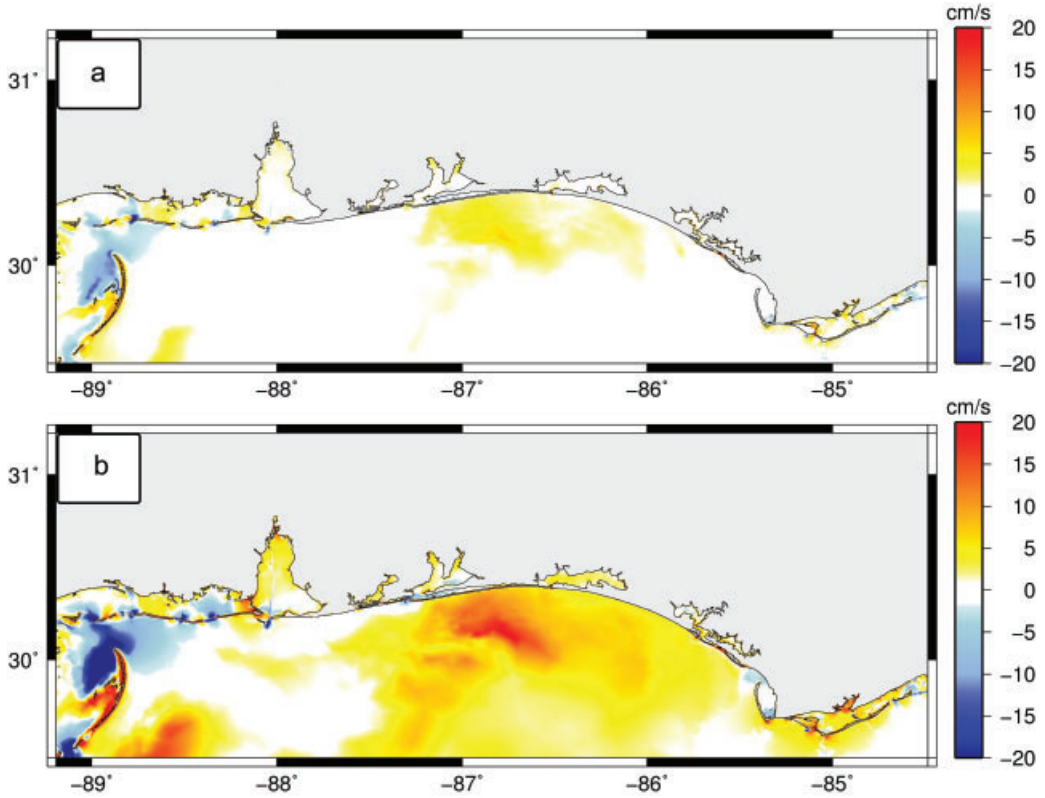

Figure 7. Changes in tidal velocities in the Northern Gulf of Mexico study area from the present scenario for (a) the 2050-high scenario and (b) the 2100-high scenario; warm colors indicate tidal velocities that have increased from the present scenario, cool colors indicate tidal velocities that have decreased from the present scenario.

The flood-ebb ratio (R), the ratio of the magnitude of the maximal flood (U_{flood}) to the maximal ebb (U_{ebb}) currents, indicates if asymmetry exists in the current velocities:

$$R = \frac{U_{\text{flood}}}{U_{\text{ebb}}} \tag{1}$$

Ratios equal to 1 indicate equal magnitudes of flood and ebb currents (no asymmetry), ratios larger than 1 indicate stronger flood currents than ebb currents (flood dominance), and ratios less than 1 indicate stronger ebb currents than flood currents (ebb dominance). The flood-ebb ratios for the present scenario for Grand Bay, Weeks Bay, and Apalachicola are illustrated in Figure 8. Tidal currents in the present scenario within Grand Bay were ebb-dominant (ratio of 0.75), whereas currents in Weeks Bay and Apalachicola were flood-dominant (ratios of 1.10 and 1.35, respectively).

The flood-ebb ratio under the future scenarios as well as the percent change in the flood-ebb ratio are summarized in Table 3. In all of the future scenarios, ebb current strengths within Weeks Bay and Apalachicola increased more than flood current strengths, resulting in a decrease in flood-dominance. In the 2050-intermediate high, 2050-high, 2100-intermediate low, 2100-intermediate high, and 2100-high scenarios, the flood-ebb ratio reversed from flood dominant to ebb dominant. SLR can change flood dominant currents to ebb dominant currents depending on the geometry of the basin and the tidal conditions [*Friedrichs et al.*, 1990; *van Maanen et al.*, 2013]. In flood dominant systems, this is because the ratio of the tidal amplitude to the water depth typically decreases with SLR [*Friedrichs et al.*, 1990]. Weeks Bay and Apalachicola had small increases in tidal amplitudes under SLR relative to the increase in water depth. In addition, the amount of intertidal area in both estuaries increased. In Grand Bay, the flood-ebb ratio increased (currents became less ebb dominant) under the lower SLR scenarios because of larger increases in the flood current velocities than the ebb current velocities. However, in the 2100-intermediate high and 2100-high scenarios, ebb current velocities increased more than flood current velocities, which

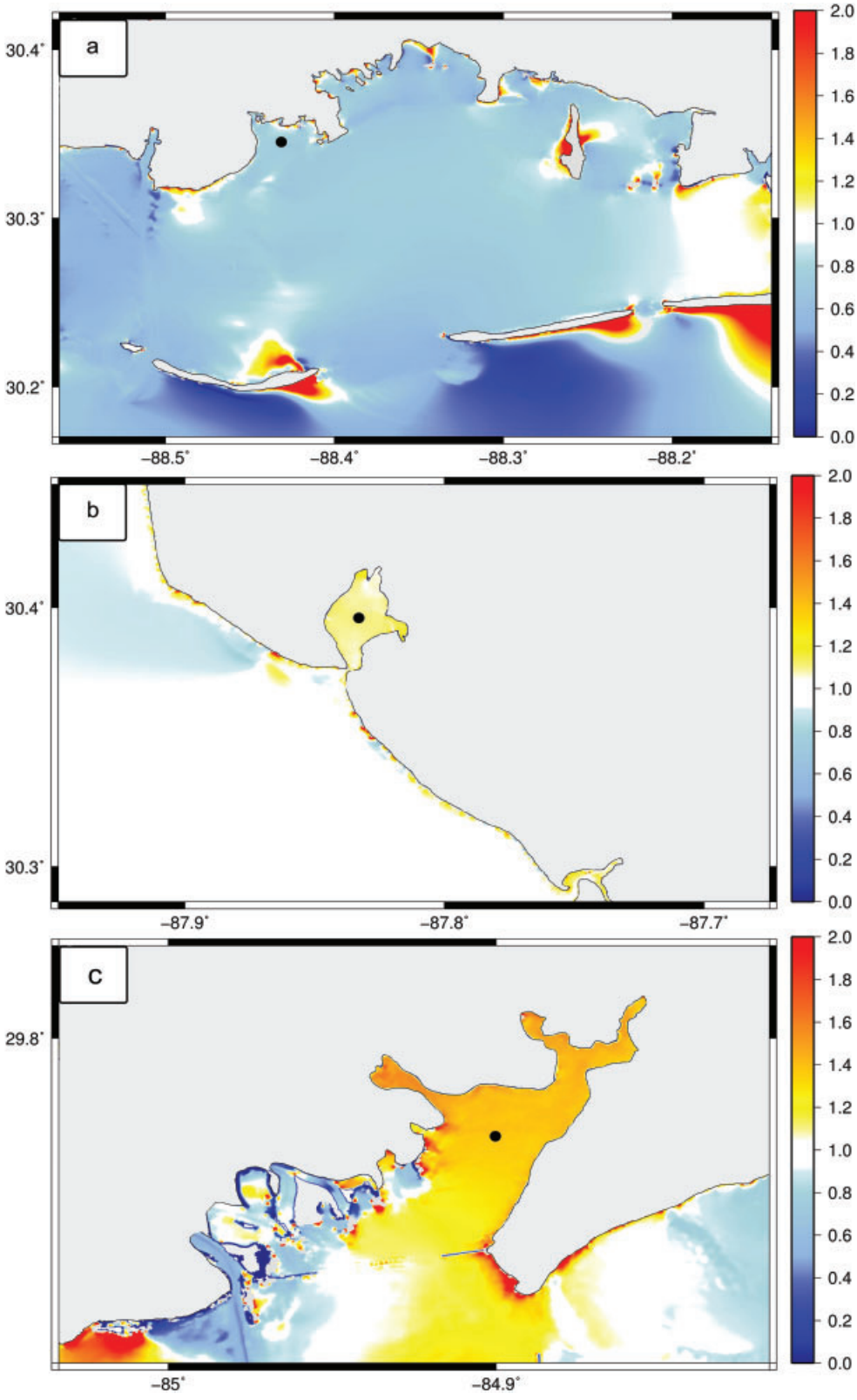

Figure 8. Flood-ebb ratios for the present scenario in (a) Grand Bay, (b) Weeks Bay, and (c) Apalachicola; at the locations marked with the black dot, flood-ebb ratios are (a) 0.75, (b) 1.10, and (c) 1.35.

Table 3. Flood-Ebb Ratio and Change in Flood-Ebb Ratio From Present to Future Scenarios in the Three NERRs in the NGOM Study Area

Location	Present	2050 Low	2050 Int. Low	2050 Int. High	2050 High	2100 Low	2100 Int. Low	2100 Int. High	2100 High
Grand Bay	0.75	0.82 (9.5%)	0.88 (17.1%)	0.90 (19.4%)	0.91 (20.9%)	0.89 (19.1%)	0.93 (24.6%)	0.63 (−16.4%)	0.63 (−15.4%)
Weeks Bay	1.10	1.03 (−6.2%)	1.02 (−7.3%)	0.93 (−15.8%)	0.87 (−20.9%)	1.03 (−6.8%)	0.90 (−18.5%)	0.89 (−19.5%)	0.81 (−26.0%)
Apalachicola	1.35	1.23 (−8.7%)	1.18 (−12.6%)	0.96 (−29.1%)	0.86 (−36.1%)	1.17 (−13.4%)	0.89 (−34.4%)	0.93 (−31.4%)	0.82 (−39.6%)

NGOM, Northern Gulf of Mexico.
The top number is the flood-ebb ratio for the given scenario, the number in parentheses is the percent change in the flood-ebb ratio from the present scenario to the given future scenario.

resulted in currents becoming more ebb dominant. This is a result of Dauphin Island and Petit Bois Island being extensively overtopped, which increased the tidal prism and altered current strengths within the Mississippi Sound.

4.4. Inundation

Tidal inundation across the barrier islands and within the floodplain increased under all of the future scenarios as a result of the higher water levels (Figure 9). Assuming no other measures were taken to prevent inundation except those described in Section 3.3, the overall floodplain inundation increased by 78.7 km^2 (1% of the total surface area of the bays in the study domain), 881.7 km^2 (12% of the total surface area of the bays in the study domain), 157.7 km^2 (2% of the total surface area of the bays in the study domain), and 1472.2 km^2 (20% of the total surface area of the bays in the study domain) in the 2050-low, 2050-high, 2100-low, and 2100-high scenarios, respectively. The majority of tidal inundation across the domain occurred in low-lying marsh land near bays or rivers. Of the three NERRs, Apalachicola had the largest increase in inundation (396 km^2, which is equivalent to 71% of the total surface area of Apalachicola Bay) in the low-lying areas surrounding the Apalachicola River and East Bay; this is the largest estuary and contains more low-lying land than Weeks Bay and Grand Bay. In addition, portions of eastern St. Joseph's Island were overtopped in the 2100-high scenario because of the projected low dune elevations. Inundation within Grand Bay also increased within the marshes by 47 km^2, or 69% of the total surface area of Grand Bay. Offshore, Petit Bois Island and Dauphin Island were extensively overtopped in the 2100-high scenario as a result of the low dune elevations in the future scenario. Weeks Bay had the least amount of increased inundation relative to the other estuaries, but still increased by 6.5 km^2 or 93% of the total surface area of the bay. Weeks Bay has less low-lying marsh areas and more developed land than Apalachicola and Grand Bay.

5. Discussion

This research improves the overall understanding of the dynamic effects of SLR on tidal hydrodynamics in microtidal environments. It is likely that other microtidal regions with low wave energy will experience similar changes in tidal hydrodynamics under SLR. In addition, this research supports a paradigm shift in the way coastal scientists and engineers model the effects of SLR [*Bilskie et al.*, 2014; *Passeri et al.*, 2015c]. Accounting for the co-evolution of morphology in conjunction with SLR allows for more comprehensive evaluations of hydrodynamics. Future efforts building upon this work could consider additional morphologic changes such as wetland variation, inlet morphology, and barrier island breaching.

These findings can be used to inform various coastal assessments of SLR. The decision-making flow chart (Figure 3) can provide direction for future hydrodynamic assessments of SLR implementing projections of morphology. Outputs in the form of future scenarios (sea levels and projections of morphology) enable storm surge assessments of SLR across the NGOM [*Bilskie et al.*, 2015c]. In addition, findings can provide insight for ecological assessments. Changes in tidal amplitudes are an important consideration for salt marshes; the governing parameters for biomass productivity are the elevation of the marsh table and the tidal range, which also dictates the marsh hydroperiod [*Morris et al.*, 2002]. The marsh hydroperiod is

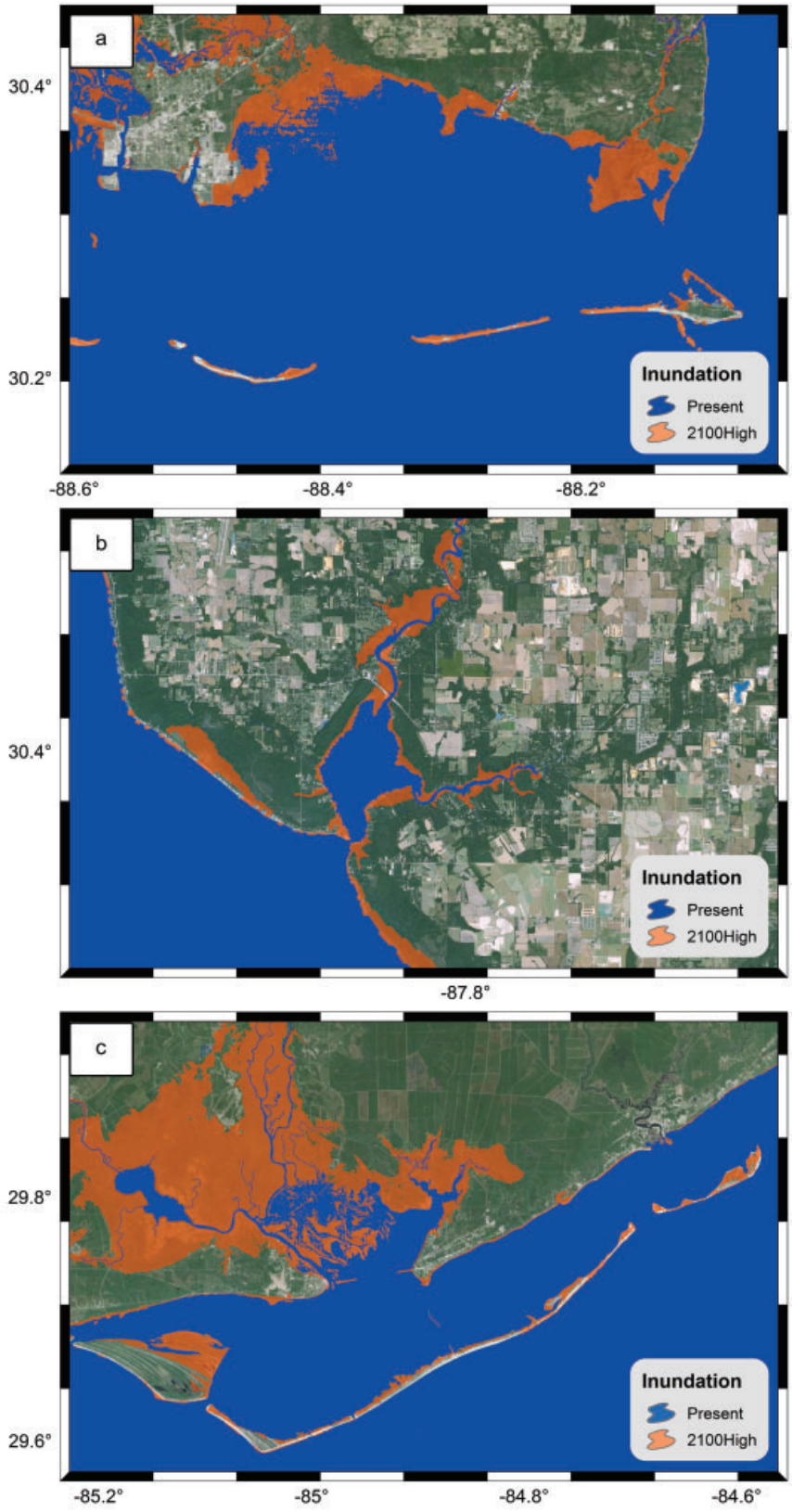

Figure 9. Tidal inundation for the present scenario and 2100-high scenario (2 m of sea level rise) for (a) Grand Bay, (b) Weeks Bay, and (c) Apalachicola.

expected to increase with SLR, which can allow for either more deposition on the marsh platform (therefore increasing productivity) or more erosion and drowning of vegetation. Microtidal marsh systems are especially sensitive to SLR because they cannot quickly adjust their mean platform elevation with respect to the tidal elevation; a relatively small increase in sea level can cause a microtidal marsh to become submerged [*Friedrichs and Perry*, 2001].

From a biological and ecological standpoint, increased flow rates can negatively affect oyster recruitment; flow rates affect larvae delivery and position maintenance during and after settlement [*Boudreaux et al.*, 2009]. This is especially important for the economy of Apalachicola Bay. Tidal asymmetries affect sediment transport in marsh tidal creeks, which can also dictate marsh sediment supply. Flood dominant tides in salt marsh creeks tend to move sediment landward, whereas ebb dominant tides tend to move sediment seaward. Flood dominant currents increase suspended sediment concentration at the creek/marsh boundary, which supplies more marine sediment to the marsh and allows for accretion on the marsh platform. Conversely, ebb dominant currents reduce the sediment supply to the marsh [*Friedrichs and Perry*, 2001]. The marshes in Grand Bay have significantly eroded historically; if the system becomes more ebb dominant under extreme SLR, marsh erosion may be exacerbated. Seagrass growth is also influenced by flood and ebb current direction [*Boer*, 2000], as tidal currents transport nutrients to seagrass beds [*Koch et al.*, 2007]. Changes in flood and ebb currents may alter the amount of sediment and nutrients in the water column, thereby affecting seagrass productivity. Projections of future shoreline positions can be used in biological studies assessing future impacts to nesting species such as sea turtles, beach mice, and shore birds.

The projected inundation areas, tidal amplitudes, and changes in tidal propagation identified in this study will be helpful in informing future navigational studies. For example, traffic patterns may be altered because of changes in shallow areas and the timing of high and low tide. Also, if the projected changes in tidal hydrodynamics increase sediment deposition in the bays, the navigational channels will require more frequent maintenance dredging.

Changes in tidal hydrodynamics are an important consideration for how natural and built communities along the NGOM may be altered in the future. In this study, SLR was found to be the primary driver of the changes in the tidal hydrodynamics, rather than morphology, which complicates adaptation strategies that may be required if SLR increases. In addition, results were based on using a single morphologic change scenario for each corresponding SLR scenario; the morphologic model actually predicted the probability of a number of morphologic outcomes in which there was increased uncertainty in shoreline change predictions under the higher SLR scenarios [*Plant et al.*, 2015]. On the contrary, dune-height predictions became more certain: they were very likely to be lower. If a different morphologic scenario was implemented in this study, the resulting shoreline change would not likely alter the hydrodynamic response as changes in tidal amplitudes and currents were driven by the higher water levels; assumptions regarding nourishment essentially prevented scenarios in which infrastructure would be lost or barrier islands would be breached. However, the uncertainty in the dune-height predictions could increase tidal inundation as a result of additional dune overtopping. In the 2100 low and intermediate-low scenarios, the uncertainty in the dune predictions has no impact on the inundation extent; if the 10th percentile of predicted dune heights was selected (i.e., in which 90% of the predicted dune heights are expected to be higher), the dunes would still be higher in elevation than mean sea level in each scenario. If the 10th percentile of predicted dune heights was selected in the 2100 intermediate-high and high scenarios, 64% and 76% of the dunes in the study area would be overtopped, as opposed to 4% and 37% when the 50th percentile was implemented, respectively. Additional overtopping not only leads to increased inundation across the shoreface but also if barrier islands became completely submerged, the flood and ebb dominance of back-bays could be altered similar to what was observed in Grand Bay as a result of Dauphin Island overtopping and altering tidal current patterns.

Lastly, results from this research can be used in management decision making and adaptation planning. Quantifying future shoreline positions and dune heights can aid in identifying erosion risks to establish monitoring, stabilization, and nourishment projects. Projections of changes in tidal amplitudes under SLR within each of the bays can assist in designing mitigation strategies, such as inlet stabilization. Areas prone to increased tidal inundation may be excluded from future development or modification and designated as protected habitats. Overall, this leads to improved coastal management decision making.

6. Conclusions

This research evaluated the integrated dynamic effects of future SLR and morphology on tidal hydrodynamics along the embayments of the NGOM, with particular focus on the Grand Bay, Weeks Bay, and Apalachicola NERRs. A large-domain hydrodynamic model modified with future SLR scenarios and projections of future morphology provided by a BN was used to simulate tidal hydrodynamics under present and future scenarios. Tidal amplitudes increased under the 2100-high scenario by as much as 67% (10.0 cm). There was a high correlation between the change in the inlet cross-sectional area and the change in the tidal amplitude in the bay. Changes in harmonic constituent phases indicated faster tidal propagation in the future scenarios in most of the bays. Tidal velocities increased in all of the NERRs under the 2100-high scenario, especially in Grand Bay where current velocities doubled. The flood-ebb velocity ratio decreased (i.e., currents became less flood dominant) by as much as 26% and 39% in all of the future scenarios within Weeks Bay and Apalachicola, respectively. Under the higher SLR scenarios, currents within both estuaries reversed from being flood dominant to ebb dominant. In Grand Bay, the flood-ebb ratio increased (i.e., currents became less ebb dominant) by as much as 25% under the lower SLR scenarios, but decreased (i.e., currents became more ebb dominant) by as much as 16% under the higher SLR as a result of the offshore barrier islands being overtopped which increased the tidal prism in the Mississippi Sound. The tidal inundation extent increased along the NGOM study area, especially along low-lying marsh areas and barrier islands with low dune elevations. Overall, this research improves the understanding of the effects of SLR on tidal hydrodynamics in microtidal environments and reinforces taking a dynamic approach and considering estimates of future morphology when modeling the effects of SLR. Results can be used in a variety of coastal studies including storm surge and ecological assessments of SLR. Ultimately, the outcomes of this research will allow coastal managers and policy makers to make more informed decisions that address the specific needs and vulnerabilities of the Apalachicola, Grand Bay, and Weeks Bay estuaries, the broader NGOM coastal system, and estuaries elsewhere with similar geomorphic and hydrodynamic conditions.

Acknowledgments

The authors wish to thank Christine Szpilka for providing post-processing resources for the simulations and Jenna Brown, Thomas Wahl, Bruce Taggart, and the anonymous reviewers for their constructive comments. This research was funded in part under Award NA10NOS4780146 from the National Oceanic and Atmospheric Administration (NOAA) Center for Sponsored Coastal Ocean Research (CSCOR) and the Louisiana Sea Grant Laborde Chair endowment. This work used the Extreme Science and Engineering Discover Environment (XSEDE), which is supported by the National Science Foundation grant ACI-1053575. Any use of trade, firm, or product names is for descriptive purposes only and does not imply endorsement by the U.S. Government. The statements and conclusions are those of the authors and do not necessarily reflect the views of NOAA-CSCOR, Louisiana Sea Grant, XSEDE, or their affiliates. All data for this paper are properly cited and referred to in the reference list.

References

Arns, A., T. Wahl, S. Dangendorf, and J. Jensen (2015), The impact of sea level rise on storm surge water levels in the northern part of the German Bight, *Coastal Eng.*, *96*, 118–131, doi:10.1016/j.coastaleng.2014.12.002.

Bilskie, M. V., S. C. Hagen, S. C. Medeiros, and D. L. Passeri (2014), Dynamics of sea level rise and coastal flooding on a changing landscape, *Geophys. Res. Lett.*, *41*(3), 927–234, doi:10.1002/2013GL058759.

Bilskie, M. V., D. Coggin, S. C. Hagen, and S. C. Medeiros (2015a), Terrain-driven unstructured mesh development through semi-automatic vertical feature extraction, *Adv. Water Resour.*, *86*(Part A), 102–118, doi:10.1016/j.advwatres.2015.09.020.

Bilskie, M. V., S. C. Hagen, S. C. Medeiros, A. T. Cox, M. Salisbury, and D. Coggin (2015b), Data and numerical analysis of astronomic tides, wind-waves, and hurricane storm surge along the northern Gulf of Mexico, *J. Geophys. Res.: Oceans*, doi:10.1002/2015JC011400.

Bilskie, M. V., S. C. Hagen, K. Alizad, S. C. Medeiros, D. L. Passeri, H. Needham, and A. Cox (2015c), Dynamic simulation and numerical analysis of hurricane storm surge under sea level rise with geomorphologic changes along the northern Gulf of Mexico, *Earth's Future*, doi:10.1002/2015EF000347.

Boer, W. F. (2000), Biomass dynamics of seagrasses and the role of mangrove vegetation as different nutrient sources for an intertidal ecosystem, *Aquat. Bot.*, *66*(3), 225–239, doi:10.1016/s0304-3770(99)00072-8.

Boudreaux, M. L., L. J. Walters, and D. Rittschoff (2009), Interactions between native barnacles, non-native barnacles and the easter oyster *Crassostrea virginica*, *Bull. Mar. Sci.*, *84*(1), 43–57.

Byrnes, M. R., J. D. Rosati, S. F. Griffee, and J. L. Berlinghoff (2012), Sediment budget: Mississippi sound barrier islands, *Rep.*, 171 pp., U.S. Army Corps of Eng., Vicksburg, Miss.

Coggin, D. (2011), A digital elevation model for Franklin, Wakulla, and Jefferson counties, *Fla. Watershed J.*, *4*(2), 5–10.

Cowell, P. J., M. J. F. Stive, A. W. Niedoroda, H. J. De Vriend, D. J. P. Swift, G. M. Kaminsky, and M. Capobianco (2003a), The coastal tract: Part 1: A conceptual approach to aggregated modelling of low-order coastal change, *J. Coastal Res.*, *19*, 812–827.

Cowell, P. J., et al. (2003b), The coastal tract. Part 2: Applications of aggregated modelling of lower-order coastal change, *J. Coastal Res.*, *19*, 828–848.

Dean, R. G., and J. Grant (1989), Development of methodology for thirty-year shoreline projections in the vicinity of beach nourishment projects, *Rep.*, Div. of Beaches and Shores, Fla. Dep. Nat. Resour., Tallahassee, Fla.

Donoghue, J. F. (2011), Sea level history of the northern Gulf of Mexico coast and sea level rise scenarios for the near future, *Clim. Change*, *107*(1–2), 17–33, doi:10.1007/s10584-011-0077-x.

Egbert, G. D., and S. Y. Erofeeva (2002), Efficient inverse modeling of barotropic ocean tides, *J. Atmos. Oceanic Technol.*, *19*, 183–204, doi:10.1175/1520-0426(2002)019<0183:eimobo>2.0.co;2.

Egbert, G. D., A. F. Bennett, and M. G. G. Foreman (1994), TOPEX/POSEIDON tides estimated using a global inverse model, *J. Geophys. Res.: Oceans*, *99*, 24821–24852, doi:10.1029/94JC01894.

Eleuterius, C. K., and G. A. Criss (1991), Pointe aux Chenes: past, present, and future perspective of erosion, *Rep.*, Phys. Oceanogr. Sect. Gulf Coast Res. Lab., Ocean Springs, Miss.

Fitzgerald, D. M., M. S. Fenster, B. A. Argow, and I. V. Buynevich (2008), Coastal impacts due to sea level rise, *Annu. Rev. Earth Planet. Sci.*, *36*, 601–647, doi:10.1146/annurev.earth.35.031306.140139.

Florida Department of Environmental Protection (2013), Apalachicola National Estuarine Research Reserve management plan, June 2013, *Rep.*, Fla. Dep. of Environ. Prot., Tallahassee, Fla.

French, J. R. (2008), Hydrodynamic modelling of estuarine flood defence realignment as an adaptive management response to sea-level rise, *J. Coastal Res.*, *24*(2B), 1–12, doi:10.2112/05-0534.1.
Friedrichs, C. T., and J. E. Perry (2001), Tidal salt marsh morphodynamics: a synthesis, *J. Coastal Res.*, *SI 27*, 7–37.
Friedrichs, C. T., D. J. Aubrey, and P. E. Speer (1990), Impacts of relative sea level rise on evolution of shallow estuaries, in *Residual Current and Long-Term Transport*, edited by R. T. Cheng, Springer-Verlag, New York.
Gutierrez, B. T., N. G. Plant, and E. R. Thieler (2011), A Bayesian network to predict coastal vulnerability to sea level rise, *J. Geophys. Res.*, *116*(FO2009), 1–15, doi:10.1029/2010JF001891.
Gutierrez, B. T., N. G. Plant, E. A. Pendleton, and E. R. Thieler (2014), Using a Bayesian network to predict shoreline change vulnerability to sea level rise for the coasts of the United States, *Rep.*, 26 pp., U.S. Geol. Surv. Open-File Rep. 2014-1083.
Hall, G. F., D. F. Hill, B. P. Horton, S. E. Engelhart, and W. R. Peltier (2013), A high-resolution study of tides in the Delaware Bay: past conditions and future scenarios, *Geophys. Res. Lett.*, *40*, 338–342, doi:10.1029/2012GL054675.
Hapke, C., and N. Plant (2010), Predicting coastal cliff erosion using a Bayesian probabilistic model, *Mar. Geol.*, *278*, 140–149, doi:10.1016/j.margeo.2010.10.001.
Intergovernmental Panel on Climate Change (2007), Climate change 2007: the physical science basis. Contribution of working group I to the fourth assessment report of the IPCC, *Rep.*, 996 pp., Cambridge Univ. Press, Cambridge, UK and New York.
Isphording, W. C. (1985), Sedimentological investigation of the Apalachicola Bay, Florida estuarine system: prepared for the Mobile District, Corps of Engineers, *Rep.*, Univ. of Ala., Tuscaloosa, Ala.
Jarrett, J. T. (1976), General investigation of tidal inlets report 3, *Rep.*, U.S. Army Eng. Waterw. Exp. Stn., Vicksburg, Miss.
Koch, E. W., J. D. Ackerman, J. Verduin, and M. van Keulen (2007), Fluid dynamics in seagrass ecology – from molecules to ecosystems, in Seagrasses: Biology, Ecology and Conservation, edited by A. W. D. Larkum, R. J. Orth, and C. M. Duarte , pp. 193–225 , Springer, The Netherlands.
Leorri, E., R. Mulligan, D. Mallinson, and A. Cearretta (2011), Sea-level rise and local tidal range changes in coastal embayments: an added complexity in developing reliable sea-level index points, *J. Integr. Coastal Zone Manage.*, *11*(3), 307–314.
Luettich, R. A., J. J. Westerink, and N. W. Scheffner (1992), ADCIRC: an advanced three-dimensional circulation model for shelves, coasts, and estuaries. I: Theory and methodology of ADCIRC-2DDI and ADCIRC-3DL, *Rep.*, U.S. Army Corps of Eng, Vicksburg, Miss.
McBride, R. A., M. R. Byrnes, and M. W. Hiland (1995), Geomorphic response-type model for barrier coastlines: a regional perspective, *Mar. Geol.*, *126*, 143–159, doi:10.1016/0025-3227(95)00070-f.
Medeiros, S. C., S. C. Hagen, J. F. Weishampel, and J. J. Angelo (2015), Adjusting lidar-derived digital terrain models in coastal marshes based on estimated above ground biomass density, *Remote Sens.*, *7*(4), 3507–3525, doi:10.3390/rs70403507.
Miller-Way, T. L., M. Dardeau, and G. Crozier (1996), Weeks Bay National Estuarine Research Reserve: an estuarine profile and bibliography, *Rep.*, Dauphin Island Sea Lab, Dauphin Island, Ala.
Mississippi Department of Marine Resources (1999), Mississippi's coastal wetlands, *Rep.*, Coastal Preserv. Program, Biloxi, Miss.
Morris, J. T., P. V. Sundareshwar, C. T. Nietch, B. Kjerfve, and D. R. Cahoon (2002), Responses of coastal wetlands to rising sea level, *Ecology*, *83*(10), 2869–2877, doi:10.1890/0012-9658(2002)083[2869:rocwtr]2.0.co;2.
Morton, R. A. (2008), Historical changes in the Mississippi-Alabama barrier-island chain and the roles of extreme storms, sea level, and human activities, *J. Coastal Res.*, *24*(6), 1587–1600, doi:10.2112/07-0953.1.
Morton, R. A., T. L. Miller, and L. J. Moore (2004), National assessment of shoreline change: Part 1: Historical shoreline changes and associated coastal land loss along the U.S. Gulf of Mexico, *Rep.*, 45 pp., U.S. Geol. Surv., St. Petersburg, Fla.
National Marine Fisheries Service (2013), . *Annual Commercial Landings Statistics. Years Queried: 2011–2012*, National Oceanic and Atmospheric Administration, Silver Spring, Md.
O'Sullivan, W. T., and G. A. Criss (1998), Continuing erosion in southeastern coastal Mississippi-Point aux Chenes Bay, West Grand Bay, Middle Bay, Grande Batture Islands: 1995–1997, in *Sixty-Second Annual Meeting of the Mississippi Academy of Sciences*, Biloxi, Miss.
Parris, A., et al. (2012), Global sea level rise scenarios for the United States National Climate Assessment, NOAA Tech Memo OAR CPO-1, pp. 37, Silver Spring, Md.
Passeri, D. L., S. C. Hagen, S. C. Medeiros, and M. V. Bilskie (2015a), Impacts of historic morphological changes and sea level rise on tidal hydrodynamics in a microtidal estuary (Grand Bay, MS), *Cont. Shelf Res.*, *111*(Part B), 150–158, doi:10.1016/j.csr.2015.08.001.
Passeri, D. L., S. C. Hagen, M. V. Bilskie, and S. C. Medeiros (2015b), On the significance of incorporating shoreline changes for evaluating coastal hydrodynamics under sea level rise scenarios, *Nat. Hazards*, *75*(2), 1599–1617, doi:10.1007/s11069-014-1386-y.
Passeri, D. L., S. C. Hagen, S. C. Medeiros, M. V. Bilskie, K. Alizad, and D. Wang (2015c), The dynamic effects of sea level rise on low gradient coastal landscapes: a review, *Earth's Future*, *3*, 159–181, doi:10.1002/2015EF000298.
Pelling, H. E., K. Uehara, and J. A. M. Green (2013), The impact of rapid coastline changes and sea level rise on the tides in the Bohai Sea, China, *J. Geophys. Res. Oceans*, *118*, 3462–3472, doi:10.1002/JGRC.20258.
Pickering, M. D., N. C. Wells, K. J. Horsburgh, and J. A. M. Green (2012), The impact of future sea-level rise on the European Shelf tides, *Cont. Shelf Res.*, *35*, 1–15, doi:10.1016/j.csr.2011.11.011.
Plant, N. G., E. R. Thieler, and D. L. Passeri (2015), Coupling long-term shoreline change to sea-level rise and coastal morphology in the Gulf of Mexico using a Bayesian network, *Earth's Future*, *4*, doi:10.1002/2015EF000331.
Rosati, J. D., and G. W. Stone (2009), Geomorphologic evolution of barrier isalnds along the Northern U.S. Gulf of Mexico and implications for engineering design in barrier restoration, *J. Coastal Res.*, *25*(1), 8–22, doi:10.2112/07-0934.1.
Sampath, D. M. R., T. Boski, P. Silva, and F. A. Martins (2011), Morphological evolution of the Guadiana estuary and intertidal zone in response to projected sea level rise and sediment supply scenarios, *J. Quat. Sci.*, *26*(2), 156–170, doi:10.1002/jqs.1434.
Seim, H. E., B. Kjerfve, and J. E. Sneed (1987), Tides of Mississippi sound and the adjacent continental shelf, *Estuarine Coastal Shelf Sci.*, *25*, 143–156, doi:10.1016/0272-7714(87)90118-1.
Thieler, E. R., and E. S. Hammar-Klose (1999), National assessment of coastal vulnerability to sea level rise: preliminary results for the U.S. Atlantic Coast, *Rep.*, U.S. Geol. Surv., Woods Hole, Mass.
Valentim, J. M., L. Vaz, N. Vaz, H. Silva, B. Duarte, I. Cacador, and J. Dias (2013), Sea level rise impact in residual circulation in Tagus estuary and Ria de Aveiro lagoon, *J. Coastal Res.*, *65*, 1981–1986, doi:10.2112/sI65-335.1.
van Maanen, B., G. Coco, K. R. Bryan, and C. T. Friedrichs (2013), Modeling the morphodynamic response of tidal embayments to sea-level rise, *Ocean Dyn.*, *63*(11–12), 1249–1262, doi:10.1007/s10236-013-0649-6.
Yates, M. L., and G. Le Cozannet (2012), Evaluating European coastal evolution using Bayesian networks, *Nat. Hazards Earth Syst. Sci.*, *12*, 1173–1177, doi:10.5194/nhess-12-1173-2012.